

All-Metal Aromatic Complexes Show High Reactivity in the Oxidation Reaction of Methane and Some Hydrocarbons

Xingbang Hu and Haoran Li*

Department of Chemistry, Zhejiang University, Hangzhou 310027, P. R. China

Received: March 7, 2007; In Final Form: June 21, 2007

The C–H activations of methane, ethane, propane, and propene catalyzed by all-metal aromatic complexes Al_4Fe were investigated. The results reveal that the rate-determining barrier of methane activation reaction with Al_4Fe is lower than that of both some well-known inorganic catalysts and some metal organic catalysts. It was found that the all-metal aromatic complexes have high reactivity for the C–H activation of ethane, propane, and propene. Further research showed that the ability of all-metal aromatic complex to accept an electron and the degree of electron delocalization on its aromatic plane had obvious influences on the reactivity of Al_4Fe . The present work predicts a new kind of catalyst for the alkyl C–H activation reaction: all-metal aromatic catalyst.

1. Introduction

The oxidation reaction is one of the most important reactions in current chemical industry, for it is a crucial way to convert hydrocarbons into more useful oxygenated compounds. However, due to the high C–H bond dissociation energy, most of the saturated carbon–hydrogen bonds are hard to oxidize. P450 enzymes are monooxygenation catalysts and highly effective for the oxidation of hydrocarbons.¹ The active center of P450 enzymes is an oxoiron heme.² Sligar et al. and Poulos et al. elucidated the structure of the active center of P450 enzymes by X-ray diffraction^{3a} and EXAFS crystallography.^{3b} Some key intermediates in the catalytic cycle of cytochrome P450 have been identified by experiments.^{3c–e} Shaik et al. confirmed these experimental results with theoretical studies. More reaction details are presented in these theoretical studies, and they are helpful for characterizing the features of experiment.^{1,2a} The key structure of P450 is Fe–porphyrin, which has been proven to be a highly effective catalyst, too.^{2c} There are two important points for Fe–porphyrin which decides its high reactivity: porphyrin can bind metal ions and porphyrin has an electron hole. The porphyrin hole is part of the oxoiron porphyrin system that can assist with the catalysis through abstraction and reshuttling of an electron from the substrate.⁴ Fe–porphyrin is a biomimetic of cytochrome P450, and it keeps high reactivity. To explore simpler catalyst with the high catalytic efficiency of Fe–porphyrin is an interesting issue.

Recently, the finding of aromaticity in aluminum clusters Al_4^{2-} has expanded the aromaticity concept into all-metal complexes.⁵ The properties of these all-metal aromatic complexes have been widely investigated, such as the geometric structure,^{5–6} molecular orbitals,^{5,7} electron density,⁸ resonance energy,⁹ and ring current and magnetism.^{6,10} It was found that molecules or clusters built by all-metal aromatic compounds have some differences from those built by organic aromatic compounds.^{9b,11} It was also found that all-metal aromatic complexes interacted with other small molecules easily in our

recent studies.¹² Besides its aromaticity, Al_4^{2-} also has strong ability to bind with transition metal elements, which will strongly influence the electronic structure of the metal. We can speculate that all-metal aromatic complexes may also have excellent reactivity in some reactions. The investigation on the reactivity of all-metal aromatic complexes is a challenging work^{5b} and development in this field is very slow,¹³ because the all-metal aromatic complexes were discovered only several years ago.^{6–12} All-metal aromatic complexes show some similar characteristics with porphyrin, such as aromaticity and the ability to bind with transition metals. Whether they have similar reactivity as metal–porphyrin is quite interesting and remains unknown.

The need for the oxidation of methane, one of the most abundant natural sources on the earth, expands quickly. How to activate methane to corresponding oxides such as methanol is a significant but challenging research in modern chemistry. The high dissociation energy (105.0 kcal/mol) of the C–H bond calls for effective catalysts. Until now, many molecules with excellent catalytic ability for methane activation reaction have already been reported. Among these, inorganic catalysts (such as V_4O_{10} ,¹⁴ Mo_3O_9 ,¹⁵ FeO^+ , MnO^+ , CuO^+ , and CoO^+ ,¹⁶ Pt-containing inorganic complexes,¹⁷ iron-substituted polyoxometalate “ $POM-Fe=O^{4-}$ ”,¹⁸ chromyl chloride;¹⁹ and gold complexes²⁰) and metal organic catalysts [such as compound I of P450,^{1,2,4,21} methane monooxygenase hydroxylase component (MMOH),²² bipyrimidine– $PtCl_2$,²³ and *N*-heterocyclic carbene Pd(II) complexes²⁴] are two kinds of the most important categories. Compared with the inorganic catalysts, the metal organic catalysts mentioned above are usually more effective and the barriers of rate-determining step catalyzed by them are lower. However, $POM-Fe=O^{4-}$ is an exception, the reactivity of which is higher than that of compound I of P450.¹⁸

The present work will explore the reactivity of all-metal aromatic complexes for the methane activation reaction, which concerns two current chemistry researches: the activation of methane and the reactivity of all-metal aromatic complexes. In order to shed more light on the reactivity of all-metal aromatic complexes, the rate-determining steps of the oxidations of ethane, propane, and propene were also investigated.

* Corresponding author. Fax: +86-571-8795-1895. E-mail: lihr@zju.edu.cn.

2. Computational Methods

Satisfying results of the methane oxidation can be obtained at with the B3LYP method.^{4,15,16d,18,22} B3LYP was also accurate enough to describe all-metal aromatic systems.^{6,9b,12b} For some of these systems, calculations at the B3LYP level are even sufficiently accurate compared with these results obtained at CCSD(T) and QCISD.^{6a,9b} Hence, all the geometries were fully optimized with *Gaussian 03* by the B3LYP method in this work. A total of four different basis sets were used in this research: basis set A, LANL2DZ basis set was used for Fe and 6-311++G** basis set for other atoms in methane activation reaction; basis set B, LANL2DZ basis set was used for Fe and 6-31G for other atoms; basis set C, CEP-121G basis set was used for Fe and 6-311++G** for other atoms; basis set D, 6-311++G** basis set was used for all atoms. Energy calculations, zero-point energies (ZPE) correction, nuclear independent chemical shift (NICS),²⁶ as well as delocalization index (DI) calculations²⁷ have been performed at the same level of theory as that used to optimize the structures. The electron configurations were calculated by the natural bond orbital (NBO) program. The ionization potential and electron affinity of all-metal aromatic compound and porphyrin have been calculated with basis set B.

The nuclear independent chemical shift (NICS) calculations were performed to predict the aromaticity of the catalysts. The value was calculated for a ghost atom that was placed at 1 Å below the center of the Al₄²⁻ plane. It has been known that a negative NICS indicates that the corresponding structure is aromatic, while a positive NICS indicates that the structure is antiaromatic.²⁶ Furthermore, some pioneering research has proven that for the aromatic ring, the more negative the NICS is, the greater the electron delocalization is.²⁸

3. Results and Discussion

3.1. Characters of All-Metal Aromatic Oxoiron Complex.

All-metal aromatic plane Al₄ was used to replace the porphyrin plane and a neutral all-metal aromatic system Al₄FeO was built (Figure 1). In Figure 1, the reactant, transition state, intermediate, and product are abbreviated as ^{3,5}Rea, ^{3,5}TS, ^{3,5}Int, and ^{3,5}Pro, respectively. The value of the left superscript means the spin multiplicity. For example, ³Rea means the reactant with a spin multiplicity of 3 (two unpaired electrons).

The calculated NICS value of Al₄²⁻ is -27.3 ppm,^{12a} which further demonstrates that the all-metal ring Al₄ is aromatic.⁵ Sola et al. have proposed that the delocalization index (DI) can be used as an electronic aromaticity criterion.²⁷ The difference of the DI of the Al–Al bond (Δ DI) was only 0.001, which suggests that electrons in the Al₄ ring are highly delocalized. High electron delocalization results in the planar structure of Al₄. When the Al₄ plane binds with Fe, the Δ DI increases a little (but still stays smaller than 0.15) for ¹Al₄Fe, ³Al₄Fe, and ⁵Al₄Fe. It indicates that binding with Fe decreases the electron delocalization of the Al₄ plane a little, but the Al₄ plane still stays aromatic because Δ DI < 0.15.^{27b} Further evidence about the aromaticity of ¹Al₄Fe, ³Al₄Fe, and ⁵Al⁵Al₄Fe comes from the NICS calculations. The calculated NICS values of ¹Al₄Fe, ³Al₄Fe, and ⁵Al₄Fe are -12.9, -19.0, and -16.9 ppm, respectively, which indicate that ¹Al₄Fe, ³Al₄Fe, and ⁵Al₄Fe are aromatic compounds. Among these three compounds, the Al₄ plane of ³Al₄Fe possesses the highest electron delocalization, which results in the most stable structure, ³Al₄FeO. It is found that ¹Al₄FeO is less stable than ³Al₄FeO and ⁵Al₄FeO by 24.4 and 20.1 kcal/mol, respectively. Hence, the reactivity of ¹Al₄FeO will not be investigated in this work.

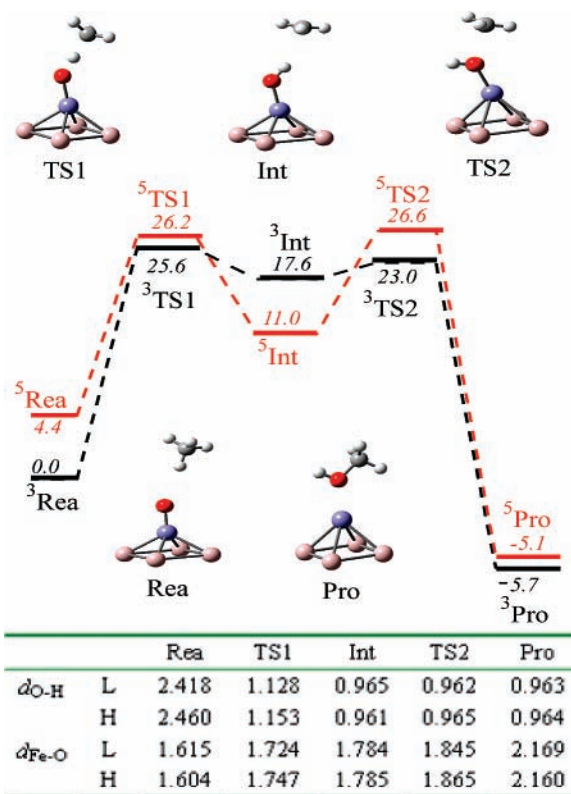


Figure 1. The reaction pathways of methane-to-methanol conversion. The italic values are Gibbs free energy changes in kcal/mol, relative to the ³Rea. Values in the table represent the bond length in Å. L means low-spin state and H means high-spin state. Calculated with basis set A.

POM–Fe=O⁴⁻,¹⁸ compound I of P450,²¹ and (N₄Py)–Fe=O²⁹ are three powerful catalysts including an Fe=O fragment for the methane oxidation. POM–Fe=O⁴⁻ is also a catalyst with an Fe=O group embedded in metal clusters. Comparison between Al₄FeO and these three catalysts is helpful for understanding the reactivity of the all-metal compound (Table 1). The Fe=O bond of ³Al₄FeO and ⁵Al₄FeO are 1.613 and 1.619 Å, and both are shorter than those of POM–Fe=O⁴⁻, compound I of P450, and (N₄Py)Fe=O. The distances from the Fe to the Al₄ plane are obviously longer than those from Fe to the porphyrin ring plane of compound I and imidazole-ligated Fe(II)–porphyrin (FePIm)³⁰ or from Fe to the plane of the four surface oxygen atoms of POM–Fe=O⁴⁻. Compared with compound I of P450, the spin densities of Al₄FeO are much closer to those of POM–Fe=O⁴⁻ and (N₄Py)Fe=O, which were found to be more powerful catalysts than compound I of P450.^{18,29}

3.2. Methane Oxidation Catalyzed by Al₄FeO. In this paper, the reaction processes with ³Al₄FeO and ⁵Al₄FeO were investigated. It was very important for understanding the reactivity of the catalysts with these two different spin states.³¹ The FeO fragment in both ³Rea and ⁵Rea carries three units of spin. The biggest difference between the ³Rea and ⁵Rea is the spin density carried by the Al₄ plane (Table 2). To conserve the spin state, the Al₄ plane of ⁵Rea carries one unit of positive spin, whereas that of ³Rea carries one unit of negative spin.

Generally, the oxidation of methane includes two steps: C–H activation and C–O rebound.⁴ Such steps for methane oxidation activated by Al₄FeO were investigated (Figure 1).

(1) C–H activation step: one hydrogen of CH₄ transfers toward the FeO fragment via a transition state TS1. TS1 exhibits a negative spin density on the migrating hydrogen (Table 2),

TABLE 1: Parameter of Catalysts Including Fe=O Fragment^a

	Al ₄ FeO: ⁵ SM (³ SM)	compd I of P450: ⁴ SM (² SM) ^b	POM-Fe=O ⁴⁻ : ⁴ SM (² SM) ^c	(N ₄ Py)Fe=O: ⁵ SM (³ SM) ^d	FePIm: ⁵ SM (³ SM) ^e
<i>r</i> (Fe–O) (Å) ^f	1.619 (1.613)	1.651 (1.648)	1.642 (1.664)	1.643 (1.651)	
<i>r</i> (Fe–plane) (Å) ^g	1.666 (1.291)	0.143 (0.154)	0.191 (0.166)		0.36 (0.14)
<i>E</i> (kcal/mol) ^h	4.3 (0.0)	0.0 (0.1)	0.0 (10.6)	4.6 (0.0)	2.8 (0.0)
SD _{Fe} ⁱ	2.76 (2.33)	1.04 (1.17)	2.15	2.93 (1.06)	
SD _O ⁱ	0.62 (0.56)	0.98 (0.92)	0.65	0.75 (0.98)	

^a The values in the parentheses belong to the low-spin state. The value of the left of “SM” means the spin multiplicity. ^b References 4a and 21a. ^c Reference 18. ^d Reference 29. ^e Reference 30. ^f Distance between Fe and O. ^g Distance between Fe and the plane, the Al₄ plane for Al₄FeO, the porphyrin ring plane for compound I of P450 or FePIm, or the plane of the four surface oxygen atoms for POM–Fe=O⁴⁻. ^h The relative energy of the high-spin state and the low-spin state. ⁱ The spin density carried by Fe and O.

TABLE 2: Spin Densities of All the States in the Methane Activation by Al₄FeO

fragment	spin ^a	Rea	TS1	Int	TS2	Pro
Al ₄	L	0.93	0.03	−0.52	0.21	0.89
	H	−0.93	−1.47	−1.73	−0.62	−0.86
Fe	L	2.51	2.92	3.21	2.97	3.02
	H	2.38	2.51	2.55	3.10	2.78
O	L	0.55	0.53	0.26	0.03	0.06
	H	0.55	0.43	0.17	0.25	0.06
H _T ^b	L	0.00	−0.01	0.07	0.03	0.01
	H	0.00	−0.03	0.03	0.00	0.01
CH ₃	L	0.00	0.52	0.98	0.76	0.02
	H	0.00	0.55	0.97	−0.72	0.00

^a L means low-spin state and H means high-spin state. ^b H_T represents the transferred proton. Calculated with basis set A.

which is a typical feature of the hydrogen abstraction process by a radical.^{4a,22e} The barrier of the C–H activation catalyzed by ⁵Al₄FeO is 21.8 kcal/mol and that by ³Al₄FeO is 25.6 kcal/mol, respectively. In the transition process Rea → TS1, to conserve the spin state, the electrons in the Al₄ plane of the high-spin process tend to pair (spin densities change from 0.93 to 0.03), whereas these electrons in the low-spin process tend to be separate (from −0.93 to −1.47). It can explain why the barrier of ³TS1 is higher than that of ⁵TS1.

(2) C–O rebound step: following the C–H activation step, it is found that the methyl migrates toward the oxygen atom via TS2. ³TS2 possesses a very low barrier (5.4 kcal/mol), whereas ⁵TS2 has a much higher rebound barrier (15.6 kcal/mol). From ³Int to ³TS2, the total spin electrons on the four 3p orbitals of Al atom increase one unit (see the electronic structure listed in the Supporting Information). As a result, the NICS value becomes more negative by 15.8 ppm in this process, which indicates that the degree of electron delocalization on the Al₄ plane of ³TS2 is higher than that of ³Int. Such an electron delocalization increasing process could compensate for the instability of the transition state; thus, the barrier of ³TS2 is very low. Correspondingly, the degree of electron delocalization changes little from ⁵Int to ⁵TS2, and ⁵TS2 possesses a higher barrier. The high barrier of ⁵TS2 suggests that the radical intermediate ⁵Int may have a longer lifetime and a greater possibility to be observed by experiment. Because the barrier of ⁵TS2 is much higher than that of ³TS2, the dominant pathway of methane activation by Al₄Fe will be the one with low spin state.

From ⁵Int to ⁵TS2, the Al₄ plane loses electrons, whereas the Al₄ plane gets electrons from ³Int to ³TS2 (Table 3). As listed in the same table, the electron-losing process will absorb energy and the electron-accepting process will release energy. This can further explain why the barrier of ³TS2 is lower than that of ⁵TS2.

During the reaction, the Al₄ almost keeps planar. The dihedral angles of the Al₄ are 0.08°, 0.06°, 0.00°, 0.38°, and 0.18° in

TABLE 3: Amount of Electron Change of the Aromatic Plane in the Reaction Processes and the Energy Change (in kcal/mol) of the Aromatic Plane Induced by Losing and Accepting an Electron

		Rea → TS1	TS1 → Int	Int → TS2	TS2 → Pro
electron change ^a	L	↑0.24	↑0.11	↑0.68	↑0.16
	H	↑0.47	↑0.24	↓0.08	↑0.45
energy change ^b	Al ₄ ²⁻ → Al ₄ ⁻	48.1	−157.1	31.3	−139.1
	Al ₄ ³⁻ → Porph ²⁻ → Porph ⁻				

^a L means low-spin state and H means high-spin state. “↑” means that the aromatic plane Al₄ gets an electron in the reaction processes and “↓” means that the aromatic plane Al₄ loses an electron. ^b Energy change of the aromatic plane losing an electron (ionization potential) or accepting an electron (electron affinity). Porph represents porphyrin. Al₄²⁻, Al₄⁻, Al₄³⁻, Porph²⁻, Porph⁻, and Porph³⁻ are all the most stable states. For example, Al₄²⁻ represents the most stable one in ¹Al₄²⁻, ³Al₄²⁻, and ⁵Al₄²⁻.

TABLE 4: Energy Changes (in kcal/mol) of Methane Activation with Different Inorganic Catalysts^a

	^L TS1	^L TS2	^H TS1	^H TS2
Al ₄ Fe	25.6 (22.5)	5.4 (1.5)	21.8 (16.0)	15.6 (9.9)
FeO ⁺ ^b	15.7	28.6	31.1	36.2
CuO ⁺ ^b	24.7	3.7	32.8	38.5
Mo ₃ O ₉ ^c	45.0	15.0	13.6	
Al ₄ Ca ^d	57.8	40.2		

^a Values in parentheses represent enthalpy changes. ^b Reference 16e. ^c Reference 15a. ^d Reference 13.

³Rea, ³TS1, ³Int, ³TS2, and ³Pro, respectively. These values are 3.98°, 0.00°, 0.83°, 0.00°, and 0.00° in ⁵Rea, ⁵TS1, ⁵Int, ⁵TS2, and ⁵Pro, respectively.

The Gibbs free energies change of Rea → Pro is −5.7 kcal/mol for the low-spin state and −9.5 kcal/mol for high-spin state, respectively. These values are lower than those catalyzed by compound I of P450 (−41.5 kcal/mol for low-spin state and −35.9 kcal/mol for high-spin state).^{4a} The low energy changes indicate that the interaction between CH₃OH and Al₄Fe is weaker than that between CH₃OH and compound I of P450, which suggests that the final product CH₃OH may leave the CH₃OH–Al₄Fe cluster by adsorbing less heat.

The C–H activation step is the rate-determining step in methane-to-methanol catalyzed by Al₄FeO, and the barrier of this step is lower than those catalyzed by some typical inorganic catalysts (Table 4), such as Mo₃O₉ (45 kcal/mol).^{15a} The C–H activation barrier catalyzed by Al₄FeO is also lower than that catalyzed by some typical organic catalysts, such as compound I of P450 (Figure 2). Though the barrier of the C–H activation step with Al₄FeO is higher than that with FeO⁺ (15.7 kcal/mol), the rate-determining step with FeO⁺ is the C–O rebound

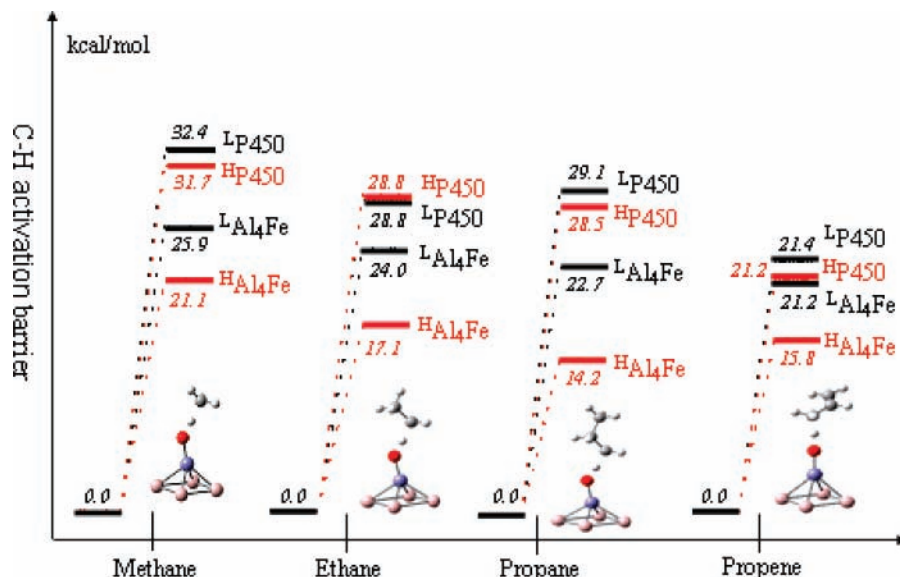


Figure 2. Alkyl C–H activation barriers (Gibbs free energy in kcal/mol) with Al₄Fe and cytochrome P450. The values with Al₄Fe are relative to the isolated reactants. Values with P450 come from ref 20b. Calculated with basis set B.

step (corresponding barrier is 28.6 kcal/mol for low-spin state and 36.2 kcal/mol for high-spin state).^{16c} Hence, the barrier of the rate-determining step with Al₄FeO is still lower than that with FeO⁺. Our previous research suggested that the aromatic plane Al₄ could also activate the oxygen molecule and oxidized oxygen can react with methane effectively; however, the corresponding barrier was quite high (57.8 kcal/mol).¹³ Hence, Al₄Fe is really a potential highly effective catalyst.

3.3. Ethane, Propane, and Propene Activation Catalyzed by Al₄FeO. Figure 2 shows the C–H activation barriers of methane, ethane, propane, and propene catalyzed by all-metal aromatic complex Al₄FeO and a typical organic aromatic catalyst, compound I of P450. From methane to ethane to propane, the barrier with Al₄Fe decreases gradually. This order is identical to that catalyzed by P450. It is worth noticing that the C–H activation barriers with Al₄Fe are all lower than those with P450. It suggests that all-metal aromatic complexes should be highly effective catalysts for the alkyl C–H activation reaction.

As indicated by a previous study, porphyrin has an electron “hole” serving as an electronic sink that can facilitate the oxidation reaction.^{4a} A similar phenomenon has also been found for Al₄²⁻. During the methane activation with Al₄Fe, the amount of electron carried by the aromatic plane Al₄ keeps increasing from ³Rea to ³Pro (Table 3). This indicates that the electron transfers from the substrate to the catalyst. As we can see, the electron affinity of all-metal aromatic plane Al₄ is greater than that of porphyrin plane, which indicates that it is more favorable for Al₄ plane to accept an electron. This can explain why the C–H activation barriers with Al₄Fe are lower than those with P450.

The C–H hydroxylation of propene catalyzed by POM–Fe=O⁴⁻ has been investigated by Shaik et al. Their calculated C–H activation barriers are 14.4–19.3 kcal/mol (values obtained with different basis sets) for the low-spin state and 12.7–17.9 kcal/mol for the high-spin state, which suggested that POM–Fe=O⁴⁻ should be a highly powerful catalyst.^{18b} For the oxidation of propene, the reactivity of Al₄FeO is much closer to POM–Fe=O⁴⁻ rather than P450.

3.4. Results with Different Calculation Methods. In order to investigate the influence of basis sets on the calculation results, four different basis sets described in the computational

TABLE 5: Barrier of TS1 (in kcal/mol) of Methane Activation with Different Basis Sets^a

	basis set A	basis set B	basis set C	basis set D
L	25.6	25.9	26.3	28.3
H	21.8	21.1	23.8	25.8

^a L means low-spin state and H means high-spin state.

method section were adopted to evaluate the barrier of methane activation. Basis sets A and B use the same basis set (LANL2DZ) for Fe but different basis sets (6-31++G** and 6-31G) for other atoms. Basis sets A, C, and D use different basis sets (LANL2DZ, CEP-121G and 6-31++G**) for Fe but the same basis (6-31++G**) for other atoms. As shown in Table 5, basis sets A and B give similar results both for low-spin state and high-spin state. This indicates that the 6-31G basis set for the atoms except Fe can well-describe the reaction. In fact, the 6-31G basis set has been widely used in the calculation of the activation processes of hydrocarbons.^{4,21} The basis set used for Fe is crucial. Basis sets including the relativistic effect (LANL2DZ and CEP-121G) of Fe give similar results; however, the basis set without the relativistic effect (6-311++G**) of Fe seems to give a higher barrier.

4. Conclusions

It seems that Al₄Fe is a powerful catalyst for the methane-to-methanol conversion. The catalytic ability of all-metal aromatic complexes is stronger than that of both some well-known inorganic catalysts and some metal organic catalysts. The present work predicts a new kind of catalyst for the alkyl C–H activation reaction: all-metal aromatic catalyst. Such a catalyst is an inorganic catalyst, however it shows some characters of metal organic catalysts, such as compound I of P450. We believe that other all-metal aromatic complexes may also have catalytic ability for the alkyl C–H activation reaction or some other reactions.

This work presented a theoretical study on the potential catalytic ability of all-metal aromatic compounds. The condition to prepare all-metal aromatic complexes is still quite rigorous⁵ and there is a long way to go to explore the reactivity of all-metal aromatic compound directly by experiment. Under this situation, theoretical predictions are especially meaningful. We

expect that this study will be helpful for the future development of the research on the reactivity of all-metal aromatic compounds. Our theoretical results are waiting for experimental support.

Shaik et al. have revealed that the reactions catalyzed by compound I of P450 in the gas phase are different from those in solution. The hydrogen bond forming between compound I and the solvent molecule in the microcosmic environment also has influence on the reaction.^{21a,32} We believe that the studies on the solvent effect will be helpful for fully understanding the reactivity of all-metal aromatic compounds. Our research in this field is in progress.

Acknowledgment. We thank the reviews for the valuable proposals and illuminating questions on the calculation and discussion. This work was supported by the National Natural Science Foundation of China (No. 20573093 and No. 20434020).

Supporting Information Available: (1) The reaction pathways of methane-to-methanol conversion ($E + ZPE$), (2) natural electron configuration, and (3) Cartesian coordinates of the optimized structures. These materials are available free of charge via the Internet at <http://pubs.acs.org>.

References and Notes

- Shaik, S.; Kumar, D.; de Visser, S. P.; Altun, A.; Thiel, W. *Chem. Rev.* **2005**, *105*, 2279.
- (a) Meunier, B.; de Visser, S. P.; Shaik, S. *Chem. Rev.* **2004**, *104*, 3947. (b) Siegbahn, P. E. M.; Blomberg, M. R. A. *Chem. Rev.* **2000**, *100*, 421. (c) Meunier, B. *Chem. Rev.* **1992**, *92*, 1411.
- (a) Schlichting, I.; Berendzen, J.; Chu, K.; Stock, A. M.; Maves, S. A.; Benson, D. E.; Sweet, R. M.; Ringe, D.; Petsko, G. A.; Sligar, S. G. *Science* **2000**, *287*, 1615. (b) Chance, M.; Powers, L.; Poulos, T.; Chance, B. *Biochemistry* **1986**, *25*, 1266. (c) Li, H.; Narashmulu, S.; Havran, L. M.; Winkler, J. D.; Poulos, T. L. *J. Am. Chem. Soc.* **1995**, *117*, 6297. (d) Atkins, W. M.; Sligar, S. G. *J. Am. Chem. Soc.* **1987**, *109*, 3754. (e) Davydov, R.; Makris, T. M.; Kofman, V.; Werst, D. E.; Sligar, S. G.; Hoffman, B. M. *J. Am. Chem. Soc.* **2001**, *123*, 1403.
- (a) Ogliaro, F.; Harris, N.; Cohen, S.; Filatov, M.; de Visser, S. P.; Shaik, S. *J. Am. Chem. Soc.* **2000**, *122*, 8977. (b) Sharma, P. K.; de Visser, S. P.; Ogliaro, F.; Shaik, S. *J. Am. Chem. Soc.* **2003**, *125*, 2291.
- (a) Li, X.; Kuznetsov, A. E.; Zhang, H. F.; Boldyrev, A. I.; Wang, L. S. *Science* **2001**, *291*, 859. (b) Boldyrev, A. I.; Wang, L. S. *Chem. Rev.* **2005**, *105*, 3716. (c) Li, Z. W.; Zhao, C. Y.; Chen, L. P. *Prog. Chem.* **2006**, *18*, 1599.
- (a) Kuznetsov, A. E.; Boldyrev, A. I.; Zhai, H. J.; Li, X.; Wang, L. S. *J. Am. Chem. Soc.* **2002**, *124*, 11791. (b) Boldyrev, A. I.; Wang, L. S. *J. Phys. Chem. A* **2001**, *105*, 10759. (c) Tsepis, C. A.; Karagiannis, E. E.; Kladou, P. F.; Tsepis, A. C. *J. Am. Chem. Soc.* **2004**, *126*, 12916.
- (a) Zubarev, D. Y.; Boldyrev, A. I.; Li, X.; Wang, L. S. *J. Phys. Chem. B* **2006**, *110*, 9743. (b) Li, Z. W.; Zhao, C. Y.; Chen, L. P. *J. Mol. Struct. (THEOCHEM)* **2007**, *809*, 45.
- (a) Santos, J. C.; Tiznado, W.; Contreras, R.; Fuentealba, P. *J. Chem. Phys.* **2004**, *120*, 1670. (b) Havenith, R. W. A.; Fowler, P. W.; Steiner, E.; Shetty, S.; Kanhere, D.; Pal, S. *Phys. Chem. Chem. Phys.* **2004**, *6*, 285.
- (a) Kuznetsov, A. E.; Boldyrev, A. I.; Li, X.; Wang, L. S. *J. Am. Chem. Soc.* **2001**, *123*, 8825. (b) Zhan, C. G.; Zheng, F.; Dixon, D. A. *J. Am. Chem. Soc.* **2002**, *124*, 14795.
- Juselius, J.; Straka, M.; Sundholm, D. *J. Phys. Chem. A* **2001**, *105*, 9939.
- (11) Hu, X. B.; Li, H. R.; Liang, W. C.; Han, S. J. *New J. Chem.* **2005**, *29*, 1295.
- (12) (a) Hu, X. B.; Li, H. R.; Liang, W. C.; Han, S. J. *Chem. Phys. Lett.* **2004**, *397*, 180. (b) Hu, X. B.; Li, H. R.; Liang, W. C.; Han, S. J. *Chem. Phys. Lett.* **2005**, *402*, 539. (c) Hu, X. B.; Li, H. R.; Wang, C. M.; Han, S. J. *Chem. Phys. Lett.* **2006**, *426*, 39.
- (13) Hu, X. B.; Li, H. R.; Wang, C. M. *J. Phys. Chem. B* **2006**, *110*, 14046.
- (14) Feyel, S.; Döbler, J.; Schröder, D.; Sauer, J.; Schwarz, H. *Angew. Chem., Int. Ed.* **2006**, *45*, 4681.
- (15) (a) Fu, G.; Xu, X.; Lu, X.; Wan, H. *J. Am. Chem. Soc.* **2005**, *127*, 3989. (b) Fu, G.; Xu, X.; Lu, X.; Wan, H. *J. Phys. Chem. B* **2005**, *109*, 6416. (c) Liang, W.; Bell, A.; Head-Gordon, M.; Chakraborty, A. *J. Phys. Chem. B* **2004**, *108*, 4362.
- (16) (a) Böhme, D. K.; Schwarz, H. *Angew. Chem., Int. Ed.* **2005**, *44*, 2336. (b) Schwarz, H. *Int. J. Mass Spectrom.* **2004**, *237*, 75. (c) Schröder, D.; Schwarz, H.; Clemmer, D. E.; Chen, Y.; Armentrout, P. B.; Baranov, V. I.; Bohme, D. K. *Int. J. Mass Spectrom. Ion Proc.* **1997**, *161*, 175. (d) Yoshizawa, K.; Shiota, Y.; Yamabe, T. *J. Am. Chem. Soc.* **1998**, *120*, 564. (e) Shiota, Y.; Yoshizawa, K. *J. Am. Chem. Soc.* **2000**, *122*, 12317. (f) Xu, X.; Faglioni, F.; Goddard, W. A., III. *J. Phys. Chem. A* **2002**, *106*, 7171.
- (17) (a) Schröder, D.; Schwarz, H. *Can. J. Chem.* **2005**, *83*, 1936. (b) Mylvaganam, K.; Bacskay, G. B.; Hush, N. S. *J. Am. Chem. Soc.* **1999**, *121*, 4633. (c) Mylvaganam, K.; Bacskay, G. B.; Hush, N. S. *J. Am. Chem. Soc.* **2000**, *122*, 2041. (d) Wolf, D. *Angew. Chem., Int. Ed.* **1998**, *37*, 3351.
- (18) (a) de Visser, S. P.; Kumar, D.; Neumann, R.; Shaik, S. *Angew. Chem., Int. Ed.* **2004**, *43*, 5661. (b) Kumar, D.; Derat, E.; Kenhin, A. M.; Neumann, R.; Shaik, S. *J. Am. Chem. Soc.* **2005**, *127*, 17712.
- (19) (a) Cook, G. K.; Mayer, J. M. *J. Am. Chem. Soc.* **1994**, *116*, 1855. (b) Cook, G. K.; Mayer, J. M. *J. Am. Chem. Soc.* **1995**, *117*, 7139.
- (20) (a) De Vos, D. E.; Sels, B. F. *Angew. Chem., Int. Ed.* **2005**, *44*, 30. (b) Jones, C.; Taube, D.; Ziatdinov, V. R.; Periana, R. A.; Nielsen, R. J.; Oxgaard, J.; Goddard, W. A., III. *Angew. Chem., Int. Ed.* **2004**, *43*, 4626.
- (21) (a) Ogliaro, F.; Cohen, S.; de Visser, S. P.; Shaik, S. *J. Am. Chem. Soc.* **2000**, *122*, 12892–12893. (b) Ogliaro, F.; de Visser, S. P.; Groves, J. T.; Shaik, S. *Angew. Chem., Int. Ed.* **2001**, *40*, 2874. (c) de Visser, S. P.; Kumar, D.; Cohen, S.; Shacham, R.; Shaik, S. *J. Am. Chem. Soc.* **2004**, *126*, 8362.
- (22) (a) Wallar, B. J.; Lipscomb, J. D. *Chem. Rev.* **1996**, *96*, 2625. (b) Baik, M. H.; Newcomb, M.; Friesner, R. A.; Lippard, S. J. *Chem. Rev.* **2003**, *103*, 2385. (c) Gherman, B. F.; Dunietz, B. D.; Whittington, D. A.; Lippard, S. J.; Friesner, R. A. *J. Am. Chem. Soc.* **2001**, *123*, 3836. (d) Basch, H.; Mogi, K.; Musaev, D. G.; Morokuma, K. *J. Am. Chem. Soc.* **1999**, *121*, 7249. (e) Guallar, V.; Gherman, B. F.; Miller, W. H.; Lippard, S. J.; Friesner, R. A. *J. Am. Chem. Soc.* **2002**, *124*, 3377. (f) Basch, H.; Musaev, D. G.; Mogi, K.; Morokuma, K. *J. Phys. Chem. A* **2001**, *105*, 3615.
- (23) Periana, R. A.; Taube, D. J.; Gamble, S.; Taube, H.; Satoh, T.; Fujii, H. *Science* **1998**, *280*, 560.
- (24) Muehlhofer, M.; Strassner, T.; Herrmann, W. A. *Angew. Chem., Int. Ed.* **2002**, *41*, 1745.
- (25) Frisch, M. J.; Trucks, G. W.; Schlegel, H. B.; Scuseria, G. E.; Robb, M. A.; Cheeseman, J. R.; Montgomery, J. A., Jr.; Vreven, T.; Kudin, K. N.; Burant, J. C.; Millam, J. M.; Iyengar, S. S.; Tomasi, J.; Barone, V.; Mennucci, B.; Cossi, M.; Scalmani, G.; Rega, N.; Petersson, G. A.; Nakatsuji, H.; Hada, M.; Ehara, M.; Toyota, K.; Fukuda, R.; Hasegawa, J.; Ishida, M.; Nakajima, T.; Honda, Y.; Kitao, O.; Nakai, H.; Klene, M.; Li, X.; Knox, J. E.; Hratchian, H. P.; Cross, J. B.; Adamo, C.; Jaramillo, J.; Gomperts, R.; Stratmann, R. E.; Yazyev, O.; Austin, A. J.; Cammi, R.; Pomelli, C.; Ochterski, J. W.; Ayala, P. Y.; Morokuma, K.; Voth, G. A.; Salvador, P.; Dannenberg, J. J.; Zakrzewski, V. G.; Dapprich, S.; Daniels, A. D.; Strain, M. C.; Farkas, O.; Malick, D. K.; Rabuck, A. D.; Raghavachari, K.; Foresman, J. B.; Ortiz, J. V.; Cui, Q.; Baboul, A. G.; Clifford, S.; Cioslowski, J.; Stefanov, B. B.; Liu, G.; Liashenko, A.; Piskorz, P.; Komaromi, I.; Martin, R. L.; Fox, D. J.; Keith, T.; Al-Laham, M. A.; Peng, C. Y.; Nanayakkara, A.; Challacombe, M.; Gill, P. M. W.; Johnson, B.; Chen, W.; Wong, M. W.; Gonzalez, C.; Pople, J. A. *Gaussian 03*, Revision B.01; Gaussian, Inc., Wallingford, CT, 2003.
- (26) (a) Schleyer, P. v. R.; Maerker, C.; Dransfeld, A.; Jiao, H.; van Eikema Hommes, N. J. R. *J. Am. Chem. Soc.* **1996**, *118*, 6317. (b) Schleyer, P. v. R. *Chem. Rev.* **2001**, *101*, 1115.
- (27) (a) Poater, J.; Sola, M.; Duran, M.; Fradera, X. *Theor. Chem. Acc.* **2002**, *107*, 362. (b) Poater, J.; Fradera, X.; Duran, M.; Sola, M. *Chem. Eur. J.* **2003**, *9*, 400. (c) Poater, J.; Duran, M.; Sola, M.; Silvi, B. *Chem. Rev.* **2005**, *105*, 3911.
- (28) Krygowski, T. M.; Cyranski, M. K. *Chem. Rev.* **2001**, *101*, 1385.
- (29) Kumar, D.; Hirao, H.; Jr., L. Q.; Shaik, S. *J. Am. Chem. Soc.* **2005**, *127*, 8026.
- (30) Ugalde, J. M.; Dunietz, B.; Dreuw, A.; Head-Gordon, M.; Boyd, R. J. *J. Phys. Chem. A* **2004**, *108*, 4653.
- (31) (a) Schröder, D.; Shaik, S.; Schwarz, H. *Acc. Chem. Res.* **2000**, *33*, 139. (b) Shaik, S.; Danovich, D.; Fiedler, A.; Schröder, D.; Schwarz, H. *Helv. Chim. Acta* **1995**, *78*, 1393.
- (32) (a) de Visser, S. P.; Shaik, S.; Sharma, P. K.; Kumar, D.; Thiel, W. *J. Am. Chem. Soc.* **2003**, *125*, 15779. (b) Hirao, H.; Kumar, D.; Thiel, W.; Shaik, S. *J. Am. Chem. Soc.* **2005**, *127*, 13007.